

HUYGENS SYNCHRONIZATION OF THREE CLOCKS EQUIDISTANT FROM EACH OTHER

EMMA D'ANIELLO¹ AND HENRIQUE M. OLIVEIRA^{2*}

ABSTRACT. This paper investigates the synchronization of three identical oscillators, or clocks, suspended from a common rigid support. We consider scenarios where each clock interacts with the other two, achieving synchronization through small impacts exchanged between oscillator pairs. The fundamental outcome of our study reveals that the ultimate synchronized state maintains a phase difference of $\frac{2\pi}{3}$ between successive clocks, either clockwise or counter-clockwise. Furthermore, these locked states exhibit an attracting set, which closure encompasses the entire initial conditions space. Our analytical approach involves constructing a nonlinear discrete dynamical system in dimension two.

These findings hold significance for sets of three weakly coupled periodic oscillators engaged in mutual symmetric impact periodic interaction, irrespective of the specific oscillator models employed. Lastly, we explore the amplitude of oscillations at the final locked state in the context of two and three interacting Andronov pendulum clocks. Our analysis reveals a precise small increase in the amplitude of the locked-state oscillations, as quantified in this paper.

1. INTRODUCTION

Synchronization among oscillators with some form of coupling is commonly referred to as universal [29] and plays a significant role in natural phenomena [10, 20, 19, 27].

In 1665, Christiaan Huygens, the inventor of the pendulum clock, made a noteworthy observation regarding synchronization between two pendulum clocks suspended from the same support [16]. While confined to bed due to illness, he witnessed both in-phase and anti-phase synchronization as the final states of the coupled system. Huygens later replicated this experiment by suspending the two clocks on a board supported by chairs.

Date: September 4, 2023.

2020 Mathematics Subject Classification. Primary 34D06, Secondary 37E30.

Key words and phrases. Synchronization of oscillators, Stability, Andronov pendulum clocks, Mutual symmetric impact interaction, Amplitude increase in locked-state oscillations.

* Corresponding author.

¹ORCID: 0000-0001-5872-0869 Dipartimento di Matematica e Fisica, Università degli Studi della Campania “Luigi Vanvitelli”, Viale Lincoln n. 5 - 81100 Caserta, Italia.

²ORCID: 0000-0002-3346-4915 Department of Mathematics and Center for Mathematical Analysis, Geometry and Dynamical Systems, Instituto Superior Técnico, University of Lisbon, Av. Rovisco Pais, 1049-001, Lisboa, Portugal .

¹emma.daniello@unicampania.it; ²holiv@math.tecnico.ulisboa.pt.

The author ED was partially supported by the program Erasmus+. The author HMO was partially supported by Fundação para a Ciéncia e Tecnologia, UIDB/04459/2020 and UIDP/04459/2020.

These distinct observations by Huygens paved the way for two separate lines of analysis as is acknowledged in [14]. The subsequent exploration involved clocks attached to a wall with momentum conservation in the clocks-beam system, allowing for the movement of the supporting plank. This line of study culminated in numerous investigations [7, 11, 12, 17, 18, 21, 25, 26, 28]. We term this model the "classical model," deeply rooted in classical mechanics and accounting for viscous friction.

In this paper, we depart from the classical model inspired by the works of Vassalo-Pereira [30] and Ralf Abraham and co-authors [1, 2], utilizing Andronov's established model for the pendulum clock with dry friction.

Our focus is the synchronization of oscillators in a plane with an asymptotically stable limit cycle. We specifically consider isochronous clocks – those with a frequency independent of amplitude. We investigate the scenario where pendulums are suspended from a rigid house beam, rendering them immobile. To approach this, we employ a perturbative model. This model accounts for the interaction between the pendulums arising from their internal impacts. The ensuing perturbation generates traveling waves that transfer kinetic energy between the oscillators.

Our study takes inspiration from a model proposed in [24]. This model introduced a theoretical framework for such interactions, accompanied by simulations and experiments involving an immobile support wall. Unlike the classical model, our approach involves discrete impacts exchanged between three identical oscillators. These impacts occur once per cycle, in the form of short burst travelling waves. We assume instantaneous coupling due to the rapid speed of mechanical waves in the medium to which the clocks are attached [24].

Our investigation reveals a symmetric asymptotic state where all clocks maintain a phase difference of $\frac{2\pi}{3}$ between each other. We term this phenomenon "Huygens synchronization," extending the concept from [1, 2, 30, 24].

The structure of this paper comprises five sections. Section 2 delves into the original pendulum clock model, briefly recapping the model for two identical clocks. In Section 3, we derive the model for three identical clocks with mutual interactions. Detailed construction information is provided in the appendix. Section 4 encompasses an analysis of the model's symmetries and stabilities. Finally, Section 5 offers conclusions and outlines potential directions for future research.

2. MODEL FOR THE SYNCHRONIZATION OF TWO OSCILLATORS

2.1. Some background. For the sake of completeness, we present a concise theory of synchronization for two oscillators exchanging small perturbations at each cycle. We focus on identical oscillators, and this theory's applicability extends to networks of identical oscillators, electronic oscillators, and various other real-world systems. In future investigations, we aim to explore cases involving slightly different oscillators, which lead to regions of stability versus instability in the parameter space, known as Arnold Tongues [9, 13, 23].

For fundamental and classical definitions and concepts related to synchronization, such as phase and frequency, we follow and refer to [27]. For broader concepts concerning the general theory of dynamical systems, such as limit cycles, we refer to [6]. Throughout this paper, we consider oscillators as dynamical systems exhibiting limit cycles. We use the term "clock" to refer to a specific type of oscillator as described by the Andronov model [24].

Given a point p_0 on the limit cycle γ , the time required for a return to p_0 after completing one cycle on the limit cycle is denoted by the period T_0 . A phase φ serves as a real coordinate describing the representative point's position on the limit cycle [22, 27].

Let B_γ represent the basin of attraction of the limit cycle. For points outside the limit cycle γ but within B_γ , we extend the phase definition as follows: all points p in B_γ that converge to the same p_0 on the limit cycle γ as $t \rightarrow \infty$ are assigned the phase φ of p_0 [15]. The set of points sharing the same phase forms an isochron curve. When oscillator states lie on the same isochron at a given time, they remain on the same isochron over time [15, 22]. In the presence of perturbations, each clock's state can deviate slightly from the limit cycle and generally jump to another isochron. We also assume that the limit cycles remain structurally stable under minor perturbations.

Considering two oscillators, labeled 1 and 2, with orbits on or near the limit cycle, each has a distinct phase, denoted φ and ψ , respectively.

Studying the synchronization of these oscillators involves establishing a dynamical system for the phase difference between them.

There are two potential research directions [27]. The first examines phase differences over continuous time, expressed as the function $\phi(t) = \psi(t) - \varphi(t)$ for $t \in [0, +\infty[$. The second, which we adopt in this paper, analyzes the discrete phase difference $\phi_n = \psi_n - \varphi_n$ at specific instances $n = 0, 1, 2, \dots$. This study exclusively employs the latter approach.

Phase synchronization occurs when the phase differences between oscillators converge toward a distinct attractor. When this attractor is a solitary point, phase locking is established. Naturally, more intricate coupled states can arise [21]. The primary objective of any synchronization theory is to derive the dynamics of this phase difference and establish the nature and existence of the attractor. In the context of Huygens' observations, the attractor was either the point 0 or the point π , and the phase dynamics remained unidimensional.

2.2. The Andronov model for an isolated clock. We revisit the model that assumes the prevalence of dry friction within the internal metal components of the clock, with viscous damping playing a secondary role. Using the angular coordinate q , the differential equation governing the isolated pendulum clock is given by

$$(1) \quad \ddot{q} + \mu \operatorname{sign} \dot{q} + q = 0,$$

where $\mu > 0$ represents the dry friction coefficient, and $\operatorname{sign}(x)$ is the classical function that takes the value -1 for $x < 0$ and 1 for $x > 0$. In [5], it was considered that during each cycle, the escape mechanism imparts a fixed amount of normalized kinetic energy $\frac{h^2}{2}$ to the pendulum, thus compensating for the kinetic energy loss caused by dry friction in each complete cycle. This transfer of kinetic energy is termed a "kick." The origin is positioned so that the kick is given precisely when $q = -\mu$. The phase portrait is depicted in Fig. 1.

Similar to [24], with initial conditions $q(t=0) = -\mu$ and $\dot{q}(t=0) = v_0$, a Poincaré section (see vol. II, page 268, of [8]) is defined as the half line $q = -\mu^+$ and $\dot{q} > 0$ [5]. The symbol $+$ indicates that we are considering the section immediately after the kick. Due to friction over a complete cycle, a velocity reduction of -4μ takes place. By evaluating the velocity, $v_n = \dot{q}(2n\pi^+)$, at the Poincaré section in

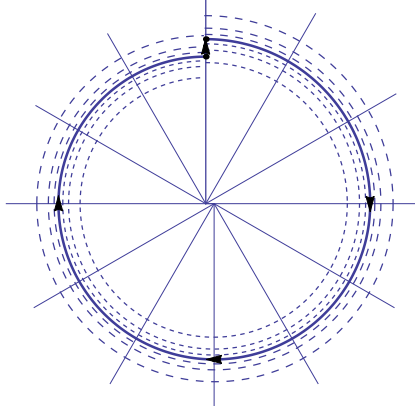


FIGURE 1. Limit cycle of an isolated clock represented as a solid curve in the phase space. The horizontal axis represents the angular position, and the vertical axis represents velocity.

each cycle, the non-linear discrete dynamical system [5] is derived as

$$(2) \quad v_{n+1} = \sqrt{(v_n - 4\mu)^2 + h^2}.$$

This equation possesses the asymptotically stable fixed point

$$(3) \quad v_f = \frac{h^2}{8\mu} + 2\mu.$$

Any initial condition $v_0 \in (4\mu, +\infty)$ converges to v_f . Each cycle corresponds to a phase increment of 2π , and the phase φ linearly varies with respect to t , specifically

$$\varphi = 2\pi t.$$

As already mentioned, the nature of limit cycle is not of fundamental importance when we consider the interaction of three identical clocks, as we shall see in the sequel. We have presented here the basis of our reasoning in the non-usual case when the computations of the limit cycle are explicit and the usual angular phase is a linear function of t .

We define the amplitude of the movement of the pendulum for the Andronov model as exactly this value v_f , which is the maximum of the angular velocity and the maximum of the angle coordinate q .

2.3. Two interacting oscillators. We briefly present the model constructed in [24] for two pendulums with the same natural frequency. When one clock receives the kick, the impact propagates in the wall slightly perturbing the second clock. The perturbation is assumed to be instantaneous since the time of travel of sound, i.e., the mechanical waves as explained in the introduction, in the wall between the clocks is assumed very small compared to the period. This reasoning allows a treatment of the three close clocks as if they were equidistant even if it is not exactly the case.

To describe and investigate the effect of the kicks, we construct a discrete dynamical system for the phase difference between the two clocks. We compute each cycle using as reference one of the clocks (the choice is irrelevant, since the model

is symmetric). We choose, to fix ideas, clock 1 as the reference: whenever its phase reaches $0 \pmod{2\pi}$, the number of cycles increases one unit from n to $n + 1$.

If there exists an attracting fixed point for that dynamical system, the phase locking occurs.

The secular repetition of perturbations leads the system with the two clocks in phase opposition as Huygens observed in 1665 [16].

In the case of frequencies equal to one and small friction coefficient, the discrete dynamical model obtained in [24] for the phase difference between two clocks, $\phi_n = \psi_n - \varphi_n$, gives the Adler equation [3, 27]

$$(4) \quad \phi_{n+1} = \phi_n + \varepsilon \sin \phi_n,$$

with a very small constant $\varepsilon = \frac{16\mu\alpha}{h^2}$, where α is a small coupling constant measuring the mutual perturbations. In the interval $[0, 2\pi[$, there are two fixed points which are π and 0 , attracting and repelling, respectively.

Equation (4) is the starting point from where we begin, in the present paper, the study the three symmetric clocks in mutual interaction.

Remark 1. *In any model with a perturbation of phase given by equation (4) per cycle, i.e., Adler's perturbation [3, 27], despite being a physical clock (with Andronov model or any different model) or other type of oscillator, electric, quantic, electronic or biological, the theory presented here for three oscillators interacting by small periodic impacts will be exactly the same, with the same conclusions.*

The amplitude of the oscillation in the case of two clocks increases slightly in the final state. We focus our analysis on the velocity at $q = -\mu^+$ and $\dot{q} = v_f$, i.e., at the Poincaré section. Since the mutual interaction affects each clock when they are in phase opposition, the equation for the Poincaré map for each generic oscillator is now

$$(5) \quad v_{n+1} = \sqrt{(v_n - 4\mu - \alpha)^2 + h^2}.$$

This equation has the asymptotically stable fixed point

$$(6) \quad v^* = \frac{(4\mu + \alpha)^2 + h^2}{2(4\mu + \alpha)}.$$

The value of v^* , which is, in fact, the maximum of the amplitude of the oscillation for the mutual interacting oscillators, is slightly greater than v_f of the isolated clock. More precisely, approximating in first order in α , and keeping in mind that h is small, we get

$$(7) \quad v^* = v_f + \left(\frac{1}{2} - \frac{h^2}{32\mu^2} \right) \alpha.$$

3. MODEL FOR THREE PENDULUM CLOCKS PLACED IN THE THREE VERTICES OF AN EQUILATERAL TRIANGLE

3.1. Hypotheses. We consider three pendulum clocks suspended at the same wall, placed in the three vertices of an equilateral triangle, say the vertices are A , B , and C and B are the extreme points of the basis of the triangles.

This geometric setting is purely conceptual. Any set of three dynamical systems receiving symmetric impacts from the other two will have the same type of response of the clocks depicted in the three vertices of an equilateral triangle.

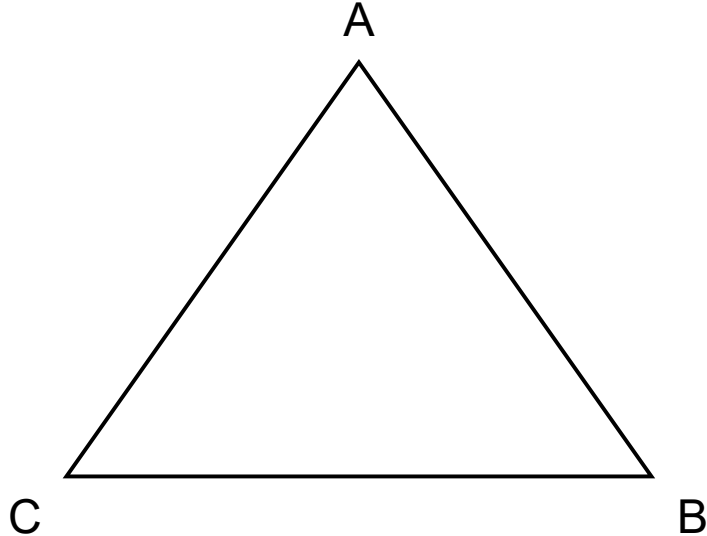


FIGURE 2. The three clocks hang at the three vertices of a triangle.

Call the clocks placed in the three vertices A , B and C , respectively, O_1 , O_2 and O_3 . When the clock A receives the kick from the escape mechanism, the impact propagates in the wall slightly perturbing the other two clocks. As in [24], the perturbation is assumed to be instantaneous, since the time of travel of sound in the wall between the clocks is assumed very small compared to the period. As for the two clocks model discussed in [24], we make the following assumptions, now formulated for three clocks.

- (1) The system has dry friction [5].
- (2) The pendulums of clocks O_1 , O_2 and O_3 have respectively natural angular frequencies $\omega_1 = \omega_2 = \omega_3 = 1$.
- (3) The perturbation in the momentum is always in the same vertical direction in the phase space [1, 2].
- (4) The friction coefficient is the same for all the three clocks, $\mu_1 = \mu_2 = \mu_3 = \mu$. The energy dissipated at each cycle of the three clocks is the same, and the energy furnished by the escape mechanism to compensate the loss of energy to friction in each cycle is $h_1 = h_2 = h_3 = h$.
- (5) The perturbative interaction is instantaneous. This is a reasonable assumption, since in general the perturbation propagation time between two clocks is several orders of magnitude lower than the periods [24].
- (6) The interaction is symmetric. The couplings have the same constant α when one clock acts on another and conversely. In this model α is assumed to be very small.
- (7) Each perturbation from clock i to clock j (where $i, j \in \{1, 2, 3\}$ with $i \neq j$), when clock i suffers its internal impact of kinetic energy h^2 , gives rise to a small perturbative change of phase which is in first order a 2π -periodic differentiable odd function P of the real variable ϕ

$$(8) \quad P(\phi) = \varepsilon \sin \phi,$$

where $\phi = \phi_{ij}$ is the phase difference between clock i and clock j .

Remark 2. The value of the constant ε in each interaction term is $\varepsilon = \frac{8\mu\alpha}{h^2}$, i.e., half of the value obtained for the two clocks [24], where μ is the dry friction coefficient, $\frac{h^2}{2}$ is the kinetic energy furnished by the internal escape mechanism of each clock once per cycle and α is the interaction coefficient between the clocks. The greater the α is, the greater the mutual influence among the clocks. In this paper, we do not need to particularize ε , since we are not interested in doing experimental computations. In this paper, we are interested in the fundamental result of symmetry between three oscillators subject to very weak mutual symmetric interaction.

Most of the reasoning is independent on the form of the function $P(\phi)$, therefore we consider a general differentiable odd function of the real variable ϕ , $P(\phi)$, for the development of the model, and consider it of the form (8) when we analyse the model in section 4.

Observe that $|\sin(x + \varepsilon \sin y) - \sin x| < \varepsilon$ when ε is assumed to be sufficiently small. Therefore, we restrict our model to first order. We consider all the values of variables and constants in IS units.

3.2. Construction of the model. We now construct a dynamical system using as reference the phase of the clock in the vertex A (= clock O_1). This reference is arbitrary: any of the clocks can be used as the reference clock with the same results at the end, since the system is symmetric. We compute the effects of all phase differences and perturbations when the clock at A makes a complete cycle returning to the initial position. Without loss of generality, we consider the next working hypotheses.

- (1) The initial phase of clock at A at $t = 0^-$ is zero, i.e., $\psi_1(0^-) = 0^-$, the minus $(-)$ superscript means that at the instant 0^- clock 1 is just about to receive the internal energy kick from its escape mechanism.
- (2) We consider that the initial phases of the three clocks are: $\psi_3(0^-) = \psi_3^0 > \psi_2(0^-) = \psi_2^0 > 0^- = \psi_1(0^-) = \psi_1^0$.
- (3) The perturbation satisfies the relation $P(x + Px) \simeq Px$ in first order.

To obtain the desired model, we need to proceed through 6 steps, starting from the following initial conditions, that is the phase differences of all pairs of clocks, and considering them at various points of the cycle of the reference clock.

In the sequel ψ_i^j denotes the phase of clock O_i at the $j - th$ step.

Next the six steps follow. We show all the details of the calculation in the Appendix.

INITIAL CONDITIONS

The phase difference between O_3 and O_1 is

$$(CA)_0 = \psi_3^0 - \psi_1^0 = \psi_3^0,$$

and the phase difference between O_1 and O_3 is symmetric, in the sense that

$$(AC)_0 = \psi_1^0 - \psi_3^0 = -\psi_3^0 = -(CA)_0.$$

The phase difference between O_2 and O_1 is

$$(BA)_0 = \psi_2^0 - \psi_1^0 = \psi_2^0$$

and the phase difference between O_1 and O_2 is

$$(AB)_0 = \psi_1^0 - \psi_2^0 = -\psi_2^0 = -(BA)_0.$$

The phase difference between O_3 and O_2 is

$$(CB)_0 = \psi_3^0 - \psi_2^0$$

and the phase difference between O_2 and O_3 is

$$(BC)_0 = \psi_2^0 - \psi_3^0 = -(CB)_0.$$

STEPS LEADING TO THE CONSTRUCTION OF THE MODEL

STEP 1: first impact. Interactions of O_1 on O_2 and of O_1 on O_3 , at $t = 0$.

When the system in position A attains phase $0 \pmod{2\pi}$ it receives a sudden supply of energy, for short “a kick”, from its escape mechanism, this kick propagates in the common support of the three clocks and reaches the other two clocks.

Now, the phase difference between O_3 and O_1 is corrected by the perturbative value P :

$$(CA)_I = (CA)_0 + P((CA)_0) = \psi_3^0 + P(\psi_3^0) = -(AC)_I,$$

where $(AC)_I$ is the phase difference between O_1 and O_3 , since P must be an odd function of the mutual phase difference.

The phase difference between O_2 and O_1 is

$$(BA)_I = (BA)_0 + P((BA)_0) = \psi_2^0 + P(\psi_2^0) = -(AB)_I.$$

The phase difference between O_3 and O_2 depends on $(CA)_I$ and $(BA)_I$ and it is

$$(CB)_I = \psi_3^0 - \psi_2^0 + P(\psi_3^0) - P(\psi_2^0) = -(CA)_I.$$

STEP 2: first natural time shift. The next clock to arrive at $2\pi^-$, from working hypothesis 3.2 (2), is the clock O_3 at vertex C . The situation right before O_3 receives its kick of energy is when the phase of this clock is $2\pi^-$.

At this point we have

$$\begin{cases} \psi_3^2 = 2\pi^- \\ \psi_1^2 = 2\pi - (\psi_3^0 + P(\psi_3^0)) \\ \psi_2^2 = 2\pi + \psi_2^0 - \psi_3^0 + P(\psi_2^0) - P(\psi_3^0). \end{cases}$$

STEP 3: second impact. Clock O_3 receives its internal kick, at the position 2π .

Now, we have

$$\begin{cases} \psi_3^3 = 2\pi \\ \psi_1^3 \simeq 2\pi - \psi_3^0 - 2P(\psi_3^0) \\ \psi_2^3 \simeq 2\pi + \psi_2^0 - \psi_3^0 + P(\psi_2^0) - P(\psi_3^0) + P(\psi_2^0 - \psi_3^0) \end{cases}$$

STEP 4: second natural time shift. The next clock to arrive at $2\pi^-$, from working hypothesis 3.2 (2), is the clock O_2 at vertex B . The situation right before O_2 receives its kick of energy is when the phase of this clock is $2\pi^-$.

Then we have

$$\begin{cases} \psi_2^4 = 2\pi^- \\ \psi_1^4 \simeq 2\pi - \psi_2^0 - P(\psi_2^0) - P(\psi_3^0) - P(\psi_2^0 - \psi_3^0) \\ \psi_3^4 \simeq 2\pi - \psi_2^0 + \psi_3^0 - P(\psi_2^0) + P(\psi_3^0) - P(\psi_2^0 - \psi_3^0). \end{cases}$$

STEP 5: third impact. Clock O_2 receives its internal energy kick. It reaches the position 2π .

Then we have

$$\begin{cases} \psi_2^5 = 2\pi \\ \psi_3^5 \simeq 2\pi - \psi_2^0 + \psi_3^0 - P(\psi_2^0) + P(\psi_3^0) - 2P(\psi_2^0 - \psi_3^0) \\ \psi_1^5 \simeq 2\pi - \psi_2^0 - 2P(\psi_2^0) - P(\psi_3^0) - P(\psi_2^0 - \psi_3^0). \end{cases}$$

STEP 6 (the final): third natural time shift. The next clock to arrive at $2\pi^-$, from working hypothesis 3.2 (2), is the clock O_1 at vertex A . The situation before O_1 receives its kick of energy is when the phase of this clock is $2\pi^-$, i.e., the cycles is complete.

At this point we are able to describe what happens to the phases after a complete cycle of the reference clock.

We have

$$\begin{cases} \psi_1^6 = 2\pi^- \\ \psi_2^6 \simeq 2\pi + \psi_2^0 + 2P(\psi_2^0) + P(\psi_3^0) + P(\psi_2^0 - \psi_3^0) \\ \psi_3^6 \simeq 2\pi + \psi_3^0 + P(\psi_2^0) + 2P(\psi_3^0) - P(\psi_2^0 - \psi_3^0). \end{cases}$$

Now, computing the phase differences after the first cycle of O_1 , we obtain

$$\begin{cases} (BA)_I = -(BA)_0 + 2P((BA)_0) + P((CA)_0) + P((BA)_0 - (CA)_0) \\ (CA)_I = ((CA)_0) + P((BA)_0) + 2P((CA)_0) - P((BA)_0 - (CA)_0) \end{cases}$$

Hence, if we set $x = BA$ and $y = CA$, we obtain the system

$$\begin{cases} x_1 = x_0 + 2P(x_0) + P(y_0) + P(x_0 - y_0) \\ y_1 = x_0 + P(x_0) + 2P(y_0) - P(x_0 - y_0). \end{cases}$$

THE MODEL

By iterating the argument above, we get, for n equal to the number of cycles described by O_1 , the discrete dynamical system:

$$\begin{cases} x_{n+1} = x_n + 2P(x_n) + P(y_n) + P(x_n - y_n) \\ y_{n+1} = y_n + P(x_n) + 2P(y_n) - P(x_n - y_n). \end{cases}$$

If we write

$$\begin{cases} \varepsilon\varphi(x, y) = 2P(x) + P(y) + P(x - y) \\ \varepsilon\gamma(x, y) = P(x) + 2P(y) + P(y - x), \end{cases}$$

then we have

$$\varphi(x, y) = \gamma(y, x),$$

and the iteration is a perturbation of the identity as

$$\begin{bmatrix} x_{n+1} \\ y_{n+1} \end{bmatrix} = \begin{bmatrix} 1 & 0 \\ 0 & 1 \end{bmatrix} \begin{bmatrix} x_n \\ y_n \end{bmatrix} + \varepsilon \begin{bmatrix} \varphi(x_n, y_n) \\ \varphi(y_n, x_n) \end{bmatrix},$$

that we can also write as

$$(9) \quad X_{n+1} = F(X_n) = X_n + \varepsilon\Omega(X_n),$$

where

$$\begin{aligned} X_{n+1} &= \begin{bmatrix} x_{n+1} \\ y_{n+1} \end{bmatrix}, \\ F(X_n) &= \begin{bmatrix} 1 & 0 \\ 0 & 1 \end{bmatrix} \begin{bmatrix} x_n \\ y_n \end{bmatrix} \end{aligned}$$

and

$$\Omega(X_n) = \begin{bmatrix} \varphi(x_n, y_n) \\ \varphi(y_n, x_n) \end{bmatrix}.$$

We now consider $P(x) = \varepsilon \sin x$, where $\varepsilon = \frac{\alpha\mu}{8h^2}$ from hypothesis 8, explicitly,

$$\begin{aligned} \varphi(x, y) &= 2 \sin x + \sin y + \sin(x - y) \\ \gamma(x, y) &= \sin x + 2 \sin y + \sin(y - x). \end{aligned}$$

4. ANALYSIS OF THE MODEL

4.1. Fixed points and local stability. In this section, we analyse the model (9) obtained in the previous section. In a nutshell, in this section, we see that the system is differentiable and invertible in $S = [0, 2\pi] \times [0, 2\pi]$ when $\varepsilon > 0$ is small. The perturbation map $\Omega(x, y)$ is periodic in \mathbb{R}^2 . This implies that the solution of the problem in the set S is a dynamical system and not the usual semi-dynamical system associated with discrete time. That will provide a reasonable simple structure to the problem of the stability of fixed points and will enable to derive global properties. Moreover, we prove that for small ε the set S is invariant for the dynamics of F , meaning that the two phase differences of oscillators O_2 and O_3 relative to oscillator O_1 stay in the interval $[0, 2\pi[$.

In particular, the map Ω has the zeros (π, π) , $(\frac{2}{3}\pi, \frac{4}{3}\pi)$ and $(\frac{4}{3}\pi, \frac{2}{3}\pi)$ in the interior of the set $S = [0, 2\pi] \times [0, 2\pi]$, which are fixed points of the model F . There are also four trivial fixed points, $(0, 0)$, $(0, 2\pi)$, $(2\pi, 0)$ and $(2\pi, 2\pi)$ at the corners of S , and the four fixed points $(0, \pi)$, $(\pi, 2\pi)$, $(2\pi, \pi)$ and $(\pi, 0)$ on the edges of S .

We now compute the Jacobian matrix $J(x, y)$ to establish the dynamical nature of the fixed points in the usual way.

We have

$$(10) \quad J(x, y) = \begin{bmatrix} 1 & 0 \\ 0 & 1 \end{bmatrix} + \varepsilon \begin{bmatrix} 2 \cos x + \cos(x - y) & -\cos(x - y) + \cos y \\ \cos x - \cos(x - y) & \cos(x - y) + 2 \cos y \end{bmatrix}.$$

We first consider the fixed points of F in the interior of S . We start with $(\frac{2}{3}\pi, \frac{4}{3}\pi)$ and $(\frac{4}{3}\pi, \frac{2}{3}\pi)$. The Jacobian is exactly the same

$$\begin{bmatrix} 1 - 3\frac{\sqrt{3}}{2}\varepsilon & 0 \\ 0 & 1 - 3\frac{\sqrt{3}}{2}\varepsilon \end{bmatrix},$$

meaning that those two points are locally asymptotically stable for ε sufficiently small.

The Jacobian matrix of F at (π, π) is

$$\begin{bmatrix} 1 - \varepsilon & -2\varepsilon \\ -2\varepsilon & 1 - \varepsilon \end{bmatrix},$$

with eigenvalues $1 - 3\varepsilon$ and $1 + \varepsilon$, which qualifies (π, π) as a saddle point. The stable manifold has direction $(1, 1)$, and the unstable manifold is tangent at (π, π) to the vector $(-1, 1)$.

We now consider now the points placed at the vertexes of S . The Jacobian matrix of F at $(0,0)$, $(0,2\pi)$, $(2\pi,0)$ and $(2\pi,2\pi)$ is, for all of them, the following

$$\begin{bmatrix} 1+3\varepsilon & 0 \\ 0 & 1+3\varepsilon \end{bmatrix},$$

which qualifies all the vertexes of S as a repellers.

On the vertical edges of S we have the fixed points $(0,\pi)$, and $(2\pi,\pi)$, at which the Jacobian matrix of F is

$$\begin{bmatrix} 1+\varepsilon & 0 \\ 2\varepsilon & 1-3\varepsilon \end{bmatrix},$$

which qualifies $(0,\pi)$, and $(2\pi,\pi)$ as saddle points. The stable manifold has the direction of the y axis and the unstable manifold is tangent at $(0,\pi)$ and $(2\pi,\pi)$ to the vector $(2,1)$.

Finally, at the horizontal edges of S we have the Jacobian matrix of F at $(\pi,0)$, and $(\pi,2\pi)$

$$\begin{bmatrix} 1-3\varepsilon & 2\varepsilon \\ 0 & 1+\varepsilon \end{bmatrix},$$

which qualifies $(\pi,0)$ and $(\pi,2\pi)$ again as saddle points. The stable manifold is the direction of the x axis and the unstable manifold is tangent at $(\pi,0)$ and $(\pi,2\pi)$ to the vector $(1,2)$.

The local analysis of the fixed points of F reveals a very symmetric picture. When $\varepsilon > 0$ is small ($0 < \varepsilon < \varepsilon_0 = \frac{1}{9}$ is good enough), F is a small perturbation of the identity, $F(\partial S) = \partial S$, the restriction of F to the boundary of S , ∂S , is a bijection (see section 4 for more details), and the Jacobian determinant of F is never null in the interior of S . Therefore, F is invertible on S .

4.2. Heteroclinic connections and invariant sets. We focus our attention on the existence of invariant subsets of S for the dynamics of F . Additionally, we below prove that S is itself an invariant set for the dynamics of F .

Recall that an heteroclinic (sometimes called a heteroclinic connection, or heteroclinic orbit) is a path in phase space which joins two different equilibrium points. In the sequel, by sa-heteroclinic, rs-heteroclinic, and ra-heteroclinic, we mean an heteroclinic orbit connecting a saddle point to an attractor, an heteroclinic orbit connecting a repeller to a saddle point, and an heteroclinic orbit connecting a repeller to an attractor, respectively.

Let F be our model map in some set T with two fixed points p and q . Let $M_u(F,p)$ and $M_s(F,q)$ be the stable manifold and the unstable manifold ([4]: pages 78, 403) of the fixed points p and q , respectively. Then, if by M we denote the heteroclinic connecting p and q , we have

$$M \subseteq M_s(F,p) \cap M_u(F,q).$$

In particular, M is invariant, the α -limit and ω -limit sets of the points of M is respectively p and q ([4]: page 331).

The other orbits, i.e., with initial conditions not in M , cannot cross the heteroclinic connections when the map F is invertible. In that case, it would be violated the injectivity of the map. In the sequel, we study the heteroclinics that connect saddle points to the attractors. Those heteroclinics determine the nature of all the flow of the dynamical system in the plane, due to the invertible nature of F .

4.2.1. *Vertical heteroclinics.* Consider the two vertical lateral edges of S , s_0 and s_1 that are the sets $s_k = \{(x, y) \in S : (x = 2k\pi) \wedge 0 \leq y \leq 2\pi\}$, $k = 0, 1$. Consider the image of these segments under F . If we write $F = (F_1, F_2)$, then

$$\begin{cases} F_1(2k\pi, y) = 2k\pi + \varepsilon \sin y + \varepsilon \sin(-y) = 2k\pi \\ F_2(2k\pi, y) = y + 2\varepsilon \sin y + \varepsilon \sin y = y + 3\varepsilon \sin y, \end{cases}$$

meaning that for ε small enough the edges s_k , $k = 0, 1$, are invariant, as already mentioned in section 2. Because of the initial conditions, on each of the edges s_k , $k = 0, 1$, the dynamics is given by

$$\begin{cases} x_{n+1} = 2k\pi, \\ y_{n+1} = y_n + 3\varepsilon \sin y_n. \end{cases}$$

For $\varepsilon < \frac{1}{9}$, the map $g : [0, 2\pi] \rightarrow [0, 2\pi]$ defined by $g(t) = t + 3\varepsilon \sin t$ is a homeomorphism from the interval $[0, 2\pi]$ into itself, as we can see in Fig. 3. Moreover, since there is an attracting fixed point of this map at π , the dynamics in the sets s_0 and s_1 can be split in two subsets where the dynamics is again invariant, which is not very important for our global discussion but establishes that the stable manifolds of the saddle points $(0, \pi)$ and $(2\pi, \pi)$ are, exactly and respectively, the sets s_0 and s_1 .

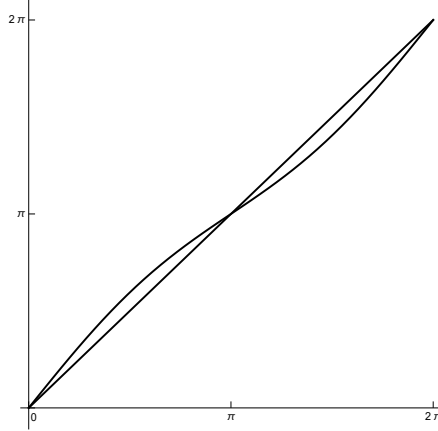


FIGURE 3. Graph of the map g , which is an homeomorphism in the interval $[0, 2\pi]$.

We have just shown that both s_0 and s_1 contain two heteroclinic connections: in s_0 , the line segment s_0^- from $(0, 0)$ to $(0, \pi)$ and s_0^+ from $(0, 2\pi)$ to $(0, \pi)$; and in s_1 , the line segment s_1^- from $(2\pi, 0)$ to $(2\pi, \pi)$ and s_1^+ from $(2\pi, 2\pi)$ to $(2\pi, \pi)$. The total number of vertical rs -heteroclinics is 4.

4.2.2. *Horizontal heteroclinics.* Consider the two horizontal top and bottom edges of S , r_0 and r_1 , that are the sets $r_k = \{(x, y) \in S : 0 \leq x \leq 2\pi \wedge (y = 2k\pi)\}$, $k = 0, 1$. Consider the image of these segments under F . As before, if we write $F = (F_1, F_2)$, then

$$\begin{cases} F_1(x, 2k\pi) = x + 3\varepsilon \sin x \\ F_2(x, 2k\pi) = 2k\pi, \end{cases}$$

meaning that, for ε small enough, the edges r_k , $k = 0, 1$, are invariant. Because of the initial conditions, on each of the edges s_k , $k = 0, 1$, the dynamics is given by

$$\begin{cases} x_{n+1} = x_n + 3\varepsilon \sin x_n \\ y_{n+1} = 2k\pi. \end{cases}$$

For $\varepsilon < \frac{1}{9}$, the map $g : [0, 2\pi] \rightarrow [0, 2\pi]$, defined by $g(t) = t + 3\varepsilon \sin t$, is the same occurred before, now involved in the dynamics in the invariant edges r_0 and r_1 . The stable manifolds of $(\pi, 0)$ and $(\pi, 2\pi)$ are again, respectively, the edges r_0 and r_1 .

Arguing as for s_0 and s_1 , we have that both, r_0 and r_1 , contain two analogous heteroclinic connections.

We have just proved, in detail, that the boundary of S is an invariant set. More is true: each edge of S is an invariant set.

Since the map F is invertible, the initial conditions in the interior of S , S^0 , cannot cross the invariant boundary $\partial S = s_0 \cup s_1 \cup r_0 \cup r_1$, meaning that S^0 is an invariant set. This means, in particular, that for equal clocks there will be no secular drift of phase differences of the three clocks, the delays and advances are contained in the set $S = [0, 2\pi] \times [0, 2\pi]$.

The total number of horizontal rs -heteroclinics is 4. The total number of rs -heteroclinics in the boundary of S is 8.

4.2.3. Diagonal heteroclinics. Finally, we now show that, S^o , the interior set of S , can be split in two subsets, S_U and S_D , U for up and D for down, where the dynamics is again invariant. Consider now the set

$$\Delta = \{(x, y) \in S : y = x, x \in [0, 2\pi]\},$$

the diagonal of S connecting $(0, 0)$ to $(2\pi, 2\pi)$. The image of a point of Δ by F is now

$$\begin{cases} F_1(x, x) = x + 3\varepsilon \sin x, \\ F_2(x, x) = x + 3\varepsilon \sin x. \end{cases}$$

Hence, the same homeomorphism g as before appears again. We repeat the same reasoning as before and deduce that Δ is invariant under F , and it splits S^o in two open sets: the triangle above it and the triangle below it. Moreover, the stable manifold of the saddle point (π, π) is the set Δ .

This also proves the existence of two heteroclinics in Δ , connecting $(0, 0)$ to (π, π) and $(2\pi, 2\pi)$ to (π, π) , respectively. The total number of rs -heteroclinics is now 10, respectively 8 on the edges and 2 on the main diagonal Δ , all of them connecting repellers to saddles.

Consider now the other diagonal of S , i.e., the set

$$\tilde{\Delta} = \{(x, y) \in S : y = 2\pi - x, x \in [0, 2\pi]\}.$$

The image of a point of $\tilde{\Delta}$ under F now is

$$\begin{cases} F_1(x, y(x)) = x + \varepsilon \sin x + \varepsilon \sin 2x, \\ F_2(x, y(x)) = 2\pi - (x + \varepsilon \sin x + \varepsilon \sin 2x). \end{cases}$$

Hence, $\tilde{\Delta}$ is invariant.

The map $h_1 : [0, 2\pi] \rightarrow [0, 2\pi]$, defined as $h_1(t) = t + \varepsilon \sin t + \varepsilon \sin 2t$, is a homeomorphism with 5 fixed points from $[0, 2\pi]$ to itself (see Fig. 4).

We repeat the same reasoning as before and deduce that the set $\tilde{\Delta}$ splits the interior set S^o again in two open sets: the triangle above and the triangle below. So, now we have split S^o in four small triangles.

There are four heteroclinic connections in $\tilde{\Delta}$, one connecting the repeller $(0, 2\pi)$ to the attractor $(\frac{2\pi}{3}, \frac{4\pi}{3})$ (ra-heteroclinic), two *sa*-heteroclinics connecting the saddle point (π, π) to the attractors $(\frac{2\pi}{3}, \frac{4\pi}{3})$ and $(\frac{4\pi}{3}, \frac{2\pi}{3})$, and, finally, the last heteroclinic on this diagonal set is the one that connects the repeller $(2\pi, 0)$ to the attractor $(\frac{4\pi}{3}, \frac{2\pi}{3})$ (ra-heteroclinic). The total number of *sa*-heteroclinics is now 2.

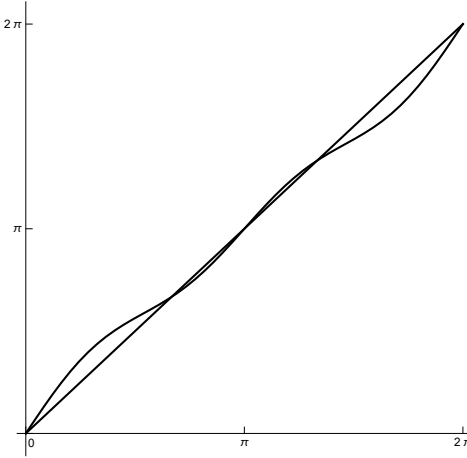


FIGURE 4. The homeomorphism h_1 with five fixed points.

We proceed with the same line of reasoning for the other *sa*-heteroclinics. Consider now the set

$$d_1 = \left\{ (x, y) \in S : y = \pi + \frac{x}{2}, x \in \left[0, \frac{2\pi}{3}\right] \right\}$$

and the map F applied to the points of d_1 :

$$\begin{cases} F_1(x, y(x)) = x + 2\varepsilon \sin x - 2\varepsilon \sin\left(\frac{x}{2}\right), \\ F_2(x, y(x)) = \pi + \frac{1}{2}(x + 2\varepsilon \sin x - 2\varepsilon \sin\left(\frac{x}{2}\right)). \end{cases}$$

The points of d_1 stay in d_1 under the action of F , proving that this set also is invariant. The function $h_2 : [0, 2\frac{\pi}{3}] \rightarrow [0, 2\frac{\pi}{3}]$, defined as $h_2(t) = t + 2\varepsilon \sin t - 2\varepsilon \sin\left(\frac{t}{2}\right)$, is a homeomorphism, from which we can readily see that the dynamics in d_1 is quite simple. The graph of this homeomorphism can be seen in Fig. 5. There is one *sa*-heteroclinic from the saddle at $(0, \pi)$ to the attractor $(\frac{2\pi}{3}, \frac{4\pi}{3})$. Actually, there is another heteroclinic in the segment connecting the repeller $(2\pi, 2\pi)$ to the attractor $(\frac{2\pi}{3}, \frac{4\pi}{3})$, but this is not an *sa*-heteroclinic. Up to now, we have 3 *sa*-heteroclinic connections.

Consider now the set $c_1 = \{(x, y) \in S : y = 2x, x \in [\frac{2\pi}{3}, \pi]\}$ and the map F applied to the points of c_1

$$\begin{aligned} F_1(x, y) &= x + \varepsilon \sin x + \varepsilon \sin 2x, \\ F_2(x, y) &= y + 2\varepsilon \sin x + 2\varepsilon \sin 2x, \end{aligned}$$

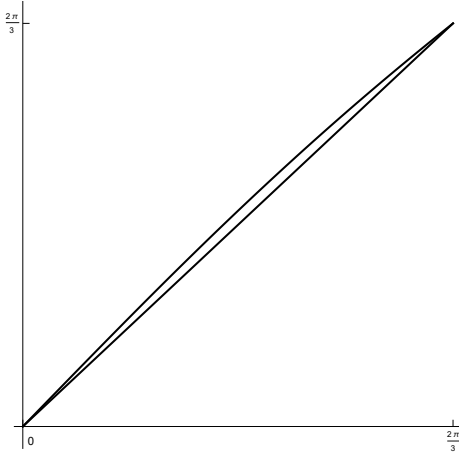


FIGURE 5. The homeomorphism h_1 with two fixed points, one repeller and the other attractor.

the points of c_1 stay in c_1 under F , proving that this set is invariant. Actually, the segment would be invariant if we extended x to the interval $[0, \pi]$, but we are not interested in heteroclinics from repellers to attractors. Moreover, the dynamics is given by a restriction of h_1 to the interval $[\frac{2\pi}{3}, \pi]$. In this interval there are only two fixed points, the attractor $\frac{2\pi}{3}$ and the repeller π . This procedure adds one more *sa*-heteroclinic to the global picture. So, we have found, up to now, 4 *sa*-heteroclinics.

In S_D , we consider

$$c_2 = \left\{ (x, y) \in S : y = 2(x - \pi), x \in \left[\pi, \frac{4\pi}{3} \right] \right\}$$

and

$$d_2 = \left\{ (x, y) \in S : y = \frac{x}{2}, x \in \left[\frac{4\pi}{3}, 2\pi \right] \right\}.$$

Following exactly the same reasoning as before, we obtain two more *sa*-heteroclinics, one connecting $(\pi, 0)$ to the attractor $(\frac{4\pi}{3}, \frac{2\pi}{3})$ and the other connecting $(2\pi, \pi)$ to the same attractor.

4.3. Phase portrait. The total number of *sa*-heteroclinics is 6. All of them are straight segments. The other 8 *sa*-heteroclinics split the set S in six invariant sets as can be seen in Fig. 6, where the red curves represent saddle-node heteroclinics. The flow curves represented in the phase portrait. Since the map F is invertible, no orbit can cross either the red curves, blue curves or black flow curves. There are only two attractors and the dynamics, due to the invertible nature of the map F and its large symmetry, is relatively simple: in every invariant set in the plane, the restriction maps are again homeomorphisms and the flow curves must follow, by continuity, the heteroclinic connections on the outer boundaries of each invariant set.

Consequently, only the orbits on the outer edges and main diagonal, i.e., in the set $s_0 \cup s_1 \cup r_0 \cup r_1 \cup d$ are not attracted to the two attractors $(\frac{2\pi}{3}, \frac{4\pi}{3})$ and $(\frac{4\pi}{3}, \frac{2\pi}{3})$. The upper attractor $(\frac{2\pi}{3}, \frac{4\pi}{3})$ attracts the points in the open upper triangle S_U with

converse results for the lower attractor $(\frac{4\pi}{3}, \frac{2\pi}{3})$ in S_D . The full picture can be seen in Fig. 6.

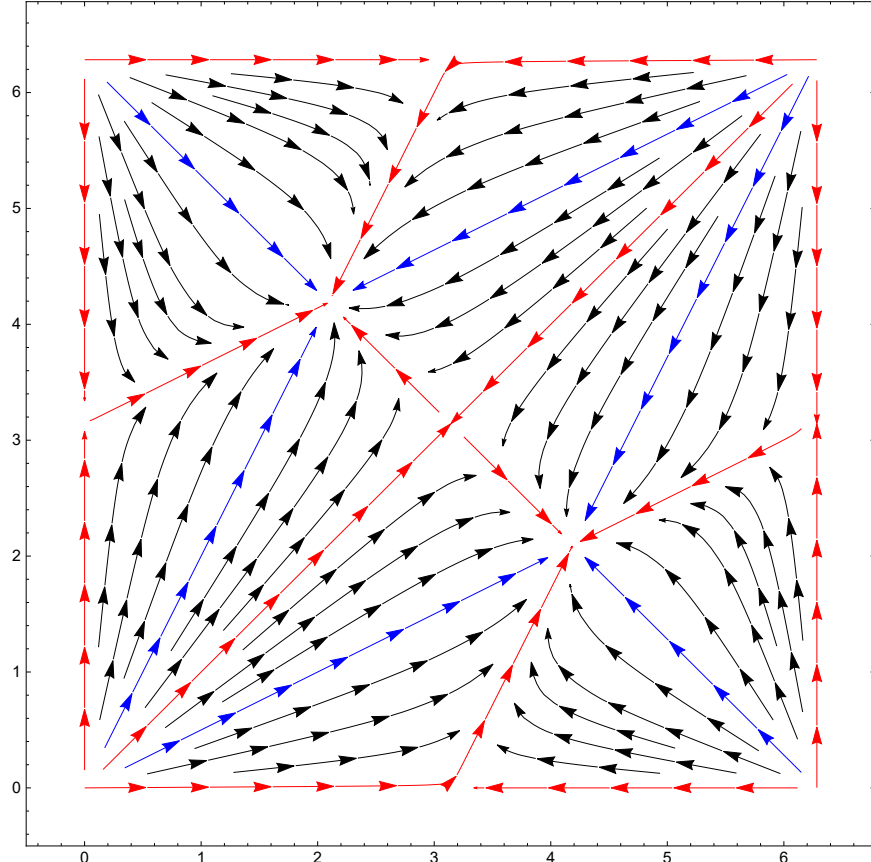


FIGURE 6. Phase portrait of F , for small ε . In red the 16 saddle-node heteroclinic connections. For illustrative purposes, we represent in blue some straight line invariant sets, actually heteroclinics, connecting repellers to attractors. All the points in the interior of S_U and S_D belong to heteroclinics connections for F .

4.4. Amplitude for three interacting oscillators in locked state. We focus again our analysis on the velocity at $q = -\mu^+$ and $\dot{q} = v_f$. Since the mutual interaction affects each clock when they are at relative phase differences of $\theta_1 = \frac{2\pi}{3}$ and $\theta_2 = \frac{4\pi}{3}$, as we can see in Fig. 7, the equation for the Poincaré map of each generic oscillator assumes now the form

$$(11) \quad v_{n+1} = \sqrt{\left(v_n - 4\mu - \alpha \sin\left(\theta_1 - \frac{\pi}{2}\right) - \alpha \sin\left(\theta_2 - \frac{\pi}{2}\right)\right)^2 + h^2}.$$

Since

$$\sin\left(\theta_1 - \frac{\pi}{2}\right) + \sin\left(\theta_2 - \frac{\pi}{2}\right) = 1,$$

this equation has again the same asymptotically stable fixed point that we have seen in equation (6), which is again slightly greater than the amplitude of the isolated clock

$$(12) \quad v^* = \frac{(4\mu + \alpha)^2 + h^2}{2(4\mu + \alpha)}.$$

The value of the maximum of the amplitude v^* is the same as in the case of two clocks.

The effect of the mutual perturbations between the clocks increases the amplitude of the oscillations, a phenomenon already observed in the experimental set up of [24].

5. CONCLUSIONS AND FUTURE WORK

In this paper we have proved that three oscillators, mutually interacting with symmetric coupling, converge to a final symmetric locked state with mutual phase differences of $\frac{2\pi}{3}$, this can happen in two different settings, clockwise or counter-clockwise, depending on the initial conditions.

This very symmetrical final locked state induces us to consider the conjecture that n oscillators weakly interacting with all the others $n - 1$ oscillators will reach a final state with mutual phase differences of $\frac{2\pi}{n}$ clockwise or counter-clockwise distributed.

In future work, already in preparation, we shall discuss the same phenomenon with slightly different natural angular frequencies ω_1 , ω_2 and ω_3 and, in particular, the existence and form of Arnold Tongues [9, 13].

As done for [24], it would be interesting to check experimentally our model, to see if the real world matches the theoretical predictions.

Disclosure of interest: The authors report no conflict of interest.

Availability of data. Not applicable.

REFERENCES

- [1] Ralph Abraham. *Phase Regulation of Coupled Oscillators and Chaos*, pages 49–78. World Scientific, Singapore, 1991.
- [2] Ralph Abraham and Alan Garfinkel. The dynamics of synchronization and phase regulation. 2003. <http://www.ralph-abraham.org/articles/Blurbs/blurb111.shtml>.
- [3] Robert Adler. A study of locking phenomena in oscillators. *Proceedings of the IRE*, 34(6):351–357, 1946.
- [4] Kathleen T. Alligood, Tim D. Sauer, and James A. Yorke. *Chaos. An introduction to dynamical systems*. Springer, 1997.
- [5] Aleksander A. Andronov, Aleksandr A. Vitt, and Semen E. Khaikin. *Theory of Oscillators*. Pergamon Press, Oxford, New York, 1959/1963/1966.
- [6] David K Arrowsmith, Colin M Place, CH Place, et al. *An introduction to dynamical systems*. Cambridge university press, 1990.
- [7] Matthew Bennett, Michael Schatz, Heidi Rockwood, and Kurt Wiesenfeld. Huygen’s clocks. *Proceedings of the Royal Society of London: Mathematics, Physical and Engineering Sciences*, 458(2019):563–579, 2002.
- [8] George David Birkhoff. *Collected Mathematical Papers*. American Mathematical Society, Providence, Rhode Island, 1950.
- [9] Philip L. Boyland. Bifurcations of circle maps: Arnol’d tongues, bistability and rotation intervals. *Comm. Math. Phys.*, 106(3):353–381, 1986.
- [10] Phablo R Carvalho and Marcelo A Savi. Synchronization and chimera state in a mechanical system. *Nonlinear Dynamics*, 102(2):907–925, 2020.

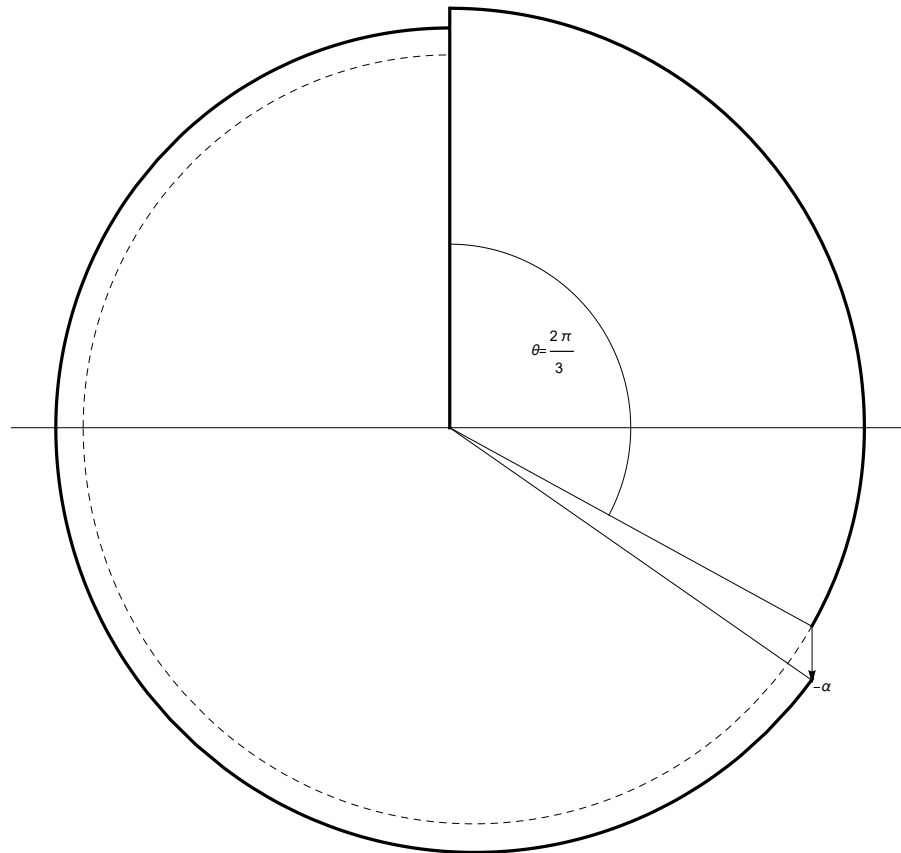


FIGURE 7. When one of the oscillators receives a perturbation near the locked state at $\frac{2\pi}{3}$ the radius of the limit cycle suffers an increase of $\alpha \sin(\frac{\pi}{6}) = \frac{\alpha}{2}$, and the amplitude suffers an increase of the same value. Each oscillator suffers two impacts per cycle, therefore the total increase of the radius, i.e., the total increase of the amplitude, is α . The effect of the perturbation is greatly exaggerated for the purpose of understandability.

- [11] Krzysztof Czolczynski, Przemyslaw Perlikowski, Andrzej Stefanski, and Tomasz Kapitaniak. Huygen's odd sympathy experiment revisited. *International Journal of Bifurcation and Chaos*, 07(21):2047–2056, 2011.
- [12] Alexander Fradkov and Boris Andrievsky. Synchronization and phase relations in the motion of two-pendulum system. *International Journal of Non-Linear Mechanics*, 6(42):895–901, 2007.

- [13] Robert Gilmore and Marc Lefranc. *The topology of chaos*. WILEY-VCH Verlag GmbH & Co. KGaA, Weinheim, Germany, 2 edition, 2011.
- [14] Guillermo H Goldsztein, Alice N Nadeau, and Steven H Strogatz. Synchronization of clocks and metronomes: A perturbation analysis based on multiple timescales. *Chaos: An Interdisciplinary Journal of Nonlinear Science*, 31(2), 2021.
- [15] John Guckenheimer. Isochrons and phaseless sets. *Journal of Mathematical Biology*, 1(3):259–273, 1975.
- [16] Christiaan Huygens. *Letters to de Sluse, Constantyn Huygens, (letters; no. 1333 of 24 February 1665, no. 1335 of 26 February 1665, no. 1345 of 6 March 1665)*. Societe Hollandaise Des Sciences, Martinus Nijho, La Haye, 1895.
- [17] Vojin Jovanovic and Sergyi Koshkin. Synchronization of huygens' clocks and the poincare method. *Journal of Sound and Vibration*, 12(331):2887–2900, 2012.
- [18] Marcin Kapitaniak, Krzysztof Czolczynski, Przemyslaw Perlikowski, Andrzej Stefanski, and Tomasz Kapitaniak. Synchronization of clocks. *Physics Reports*, 1(517):1–69, 2012.
- [19] Albert C. J. Luo. *Discrete Systems Synchronization*, pages 197–236. Springer New York, New York, NY, 2013.
- [20] Albert C.J. Luo. A theory for synchronization of dynamical systems. *Communications in Nonlinear Science and Numerical Simulation*, 14(5):1901 – 1951, 2009.
- [21] Erik Andreas Martens, Shashi Thutupalli, Antoine Fourrière, and Oskar Hallatschek. Chimera states in mechanical oscillator networks. *Proceedings of the National Academy of Sciences*, 26(110):10563–10567, 2013.
- [22] Hiroya Nakao. Phase reduction approach to synchronisation of nonlinear oscillators. *Contemporary Physics*, 57(2):188–214, 2016.
- [23] Henrique M. Oliveira and Sara Perestrelo. Stability of coupled huygens oscillators. *Journal of Difference Equations and Applications*, 28(10):1362–1380, 2022.
- [24] Henrique Manuel Oliveira and Luís Viseu Melo. Huygens synchronization of two clocks. *Scientific Reports*, 5(11548):1–12, 2015. doi: 10.1038/srep11548.
- [25] Ward T. Oud, Henk Nijmeijer, and Alexander Yu. Pogromsky. *A study of Huijgens' synchronization: experimental results*, volume 336 of *Lecture Notes in Control and Information Science*, pages 191–203. Springer, Berlin Heidelberg, 2006.
- [26] Jonatan Peña Ramirez, Luis Alberto Olvera, Henk Nijmeijer, and Joaquin Alvarez. The sympathy of two pendulum clocks: beyond huygens' observations. *Scientific reports*, 6(1):23580, 2016.
- [27] Arkady Pikovsky, Michael Rosenblum, and Jürgen Kurths. *Synchronization: A Universal Concept in Nonlinear Sciences*, volume 12 of *Cambridge Nonlinear Science Series*. Cambridge University Press, Cambridge, 1 edition, 5 2003.
- [28] Martin Senator. Synchronization of two coupled escapement-driven pendulum clocks. *Journal of sound and vibration*, 3–5(291):566–603, 2006.
- [29] Steven Strogatz. *Sync: The emerging science of spontaneous order*. Penguin UK, 2004.
- [30] José Vassalo-Pereira. A theorem on phase-locking in two interacting clocks (the Huygens effect). In André Avez, Austin Blaquiére, and Angelo Marzollo, editors, *Dynamical Systems and Micromechanics: Geometry and Mechanics*, pages 343–352, New York, London, 1982. Academic Press.

APPENDIX

The steps in the construction of the model. STEP 1: first impact. Interactions of O_1 on O_2 and of O_1 on O_3 , at $t = 0$.

When the system in position A attains phase $0 \pmod{2\pi}$ it receives a sudden supply of energy, for short “a kick”, from its escape mechanism, this kick propagates in the common support of the three clocks and reaches the other two clocks.

Now, the phase difference between O_3 and O_1 is corrected by the perturbative value P :

$$(CA)_I = (CA)_0 + P((CA)_0) = \psi_3^0 + P(\psi_3^0).$$

The phase difference between O_1 and O_3 is

$$(AC)_I = (AC)_0 + P((AC)_0) = -\psi_3^0 + P(-\psi_3^0) = -(CA)_I,$$

since P must be an odd function of the mutual phase difference.

The phase difference between O_2 and O_1 is

$$(BA)_I = (BA)_0 + P((BA)_0) = \psi_2^0 + P(\psi_2^0),$$

and the symmetric phase difference between O_1 and O_2 is

$$(AB)_I = (AB)_0 + P((AB)_0) = -\psi_2^0 + P(-\psi_2^0) = -(BA)_I.$$

The phase difference between O_3 and O_2 depends on $(CA)_I$ and $(BA)_I$ and it is

$$(CB)_I = (CA)_I - (BA)_I = \psi_3^0 - \psi_2^0 + P(\psi_3^0) - P(\psi_2^0) = -(CA)_I,$$

STEP 2: first natural time shift. The next clock to arrive at $2\pi^-$, from working hypothesis 3.2 (2), is the clock O_3 at vertex C . The situation right before O_3 receives its kick of energy is when the phase of this clock is $2\pi^-$.

At this point we have

$$\begin{cases} \psi_3^2 = 2\pi^- \\ \psi_1^2 = 2\pi - (CA)_I = 2\pi + (AC)_I = 2\pi - (\psi_3^0 + P(\psi_3^0)) \\ \psi_2^2 = 2\pi - (CB)_I = 2\pi + (BC)_I = 2\pi + \psi_2^0 - \psi_3^0 + P(\psi_2^0) - P(\psi_3^0). \end{cases}$$

STEP 3: second impact. Clock O_3 receives its internal kick, at the position 2π .

Now, we have

$$\begin{cases} \psi_3^3 = 2\pi \\ \psi_1^3 = \psi_1^2 + P(\psi_1^2) \\ = 2\pi - (\psi_3^0 + P(\psi_3^0)) + P(2\pi - (\psi_3^0 + P(\psi_3^0))) \\ = 2\pi - (\psi_3^0 + P(\psi_3^0)) - P(\psi_3^0 + P(\psi_3^0)) \\ \simeq 2\pi - \psi_3^0 - 2P(\psi_3^0) \\ \psi_2^3 = \psi_2^2 + P(\psi_2^2) \\ = 2\pi + \psi_2^0 - \psi_3^0 + P(\psi_2^0) - P(\psi_3^0) \\ + P(2\pi + \psi_2^0 - \psi_3^0 + P(\psi_2^0) - P(\psi_3^0)) \\ = 2\pi + \psi_2^0 - \psi_3^0 + P(\psi_2^0) - P(\psi_3^0) \\ + P(\psi_2^0 - \psi_3^0 + P(\psi_2^0) - P(\psi_3^0)) \\ \simeq 2\pi + \psi_2^0 - \psi_3^0 + P(\psi_2^0) - P(\psi_3^0) + P(\psi_2^0 - \psi_3^0) \end{cases}$$

STEP 4: second natural time shift. The next clock to arrive at $2\pi^-$, from working hypothesis 3.2 (2), is the clock O_2 at vertex B . The situation right before O_2 receives its kick of energy is when the phase of this clock is $2\pi^-$.

Then we have

$$\begin{cases} \psi_2^4 = 2\pi^- \\ \psi_1^4 = \psi_1^3 + 2\pi - \psi_2^3 \\ \simeq 2\pi - \psi_3^0 - 2P(\psi_3^0) + 2\pi \\ - (2\pi + \psi_2^0 - \psi_3^0 + P(\psi_2^0) - P(\psi_3^0) + P(\psi_2^0 - \psi_3^0)) \\ = 2\pi - \psi_2^0 - P(\psi_2^0) - P(\psi_3^0) - P(\psi_2^0 - \psi_3^0) \\ \psi_3^4 = \psi_3^3 + 2\pi - \psi_2^3 \\ \simeq 2\pi + 2\pi - (2\pi + \psi_2^0 - \psi_3^0 + P(\psi_2^0) - P(\psi_3^0) + P(\psi_2^0 - \psi_3^0)) \\ \simeq 2\pi - \psi_2^0 + \psi_3^0 - P(\psi_2^0) + P(\psi_3^0) - P(\psi_2^0 - \psi_3^0). \end{cases}$$

STEP 5: third impact. Clock O_2 receives its internal energy kick. It reaches the position 2π .

Then we have

$$\left\{ \begin{array}{l} \psi_2^5 = 2\pi \\ \psi_3^5 = \psi_3^4 + P(\psi_3^4) \\ \quad \simeq 2\pi - \psi_2^0 + \psi_3^0 - P(\psi_2^0) + P(\psi_3^0) - P(\psi_2^0 - \psi_3^0) \\ \quad + P(2\pi - \psi_2^0 + \psi_3^0 - P(\psi_2^0) + P(\psi_3^0) - P(\psi_2^0 - \psi_3^0)) \\ \quad \simeq 2\pi - \psi_2^0 + \psi_3^0 - P(\psi_2^0) + P(\psi_3^0) - P(\psi_2^0 - \psi_3^0) - P(\psi_2^0 - \psi_3^0) \\ = 2\pi - \psi_2^0 + \psi_3^0 - P(\psi_2^0) + P(\psi_3^0) - 2P(\psi_2^0 - \psi_3^0) \\ \psi_1^5 = \psi_1^4 + P(\psi_1^4) \\ \quad \simeq 2\pi - \psi_2^0 - P(\psi_2^0) - P(\psi_3^0) - P(\psi_2^0 - \psi_3^0) + \\ \quad P(2\pi - \psi_2^0 - P(\psi_2^0) - P(\psi_3^0) - P(\psi_2^0 - \psi_3^0)) \\ \quad \simeq 2\pi - \psi_2^0 - P(\psi_2^0) - P(\psi_3^0) - P(\psi_2^0 - \psi_3^0) - P(\psi_2^0) \\ = 2\pi - \psi_2^0 - 2P(\psi_2^0) - P(\psi_3^0) - P(\psi_2^0 - \psi_3^0). \end{array} \right.$$

STEP 6 (the final): third natural time shift. The next clock to arrive at $2\pi^-$, from working hypothesis 3.2 (2), is the clock O_1 at vertex A . The situation before O_1 receives its kick of energy is when the phase of this clock is $2\pi^-$, i.e., the cycles is complete.

At this point we are able to describe what happens to the phases after a complete cycle of the reference clock.

We have

$$\left\{ \begin{array}{l} \psi_1^6 = 2\pi^- \\ \psi_2^6 = \psi_2^5 + 2\pi - \psi_1^5 \\ \quad \simeq 2\pi + 2\pi - (2\pi - \psi_2^0 - 2P(\psi_2^0) - P(\psi_3^0) - P(\psi_2^0 - \psi_3^0)) \\ = 2\pi + \psi_2^0 + 2P(\psi_2^0) + P(\psi_3^0) + P(\psi_2^0 - \psi_3^0); \\ \psi_3^6 = \psi_3^5 + 2\pi - \psi_1^5 \\ \quad \simeq 2\pi - \psi_2^0 + \psi_3^0 - P(\psi_2^0) + P(\psi_3^0) - 2P(\psi_2^0 - \psi_3^0) + 2\pi \\ \quad - (2\pi - \psi_2^0 - 2P(\psi_2^0) - P(\psi_3^0) - P(\psi_2^0 - \psi_3^0)) \\ = 2\pi + \psi_3^0 + P(\psi_2^0) + 2P(\psi_3^0) - P(\psi_2^0 - \psi_3^0). \end{array} \right.$$

Now, we compute the phase differences after the first cycle of O_1 .
We have

$$\begin{aligned} (BA)_I &= -(AB)_I = \psi_2^6 - \psi_1^6 \\ &\simeq 2\pi + \psi_2^0 + 2P(\psi_2^0) + P(\psi_3^0) + P(\psi_2^0 - \psi_3^0) - 2\pi \\ &= \psi_2^0 + 2P(\psi_2^0) + P(\psi_3^0) + P(\psi_2^0 - \psi_3^0) \\ &= (BA)_0 + 2P((BA)_0) + P((CA)_0) + P((BA)_0 - (CA)_0) \end{aligned}$$

and

$$\begin{aligned}
 (CA)_I &= -(AC)_I = \psi_3^6 - \psi_1^6 \\
 &= 2\pi + \psi_3^0 + P(\psi_2^0) + 2P(\psi_3^0) - P(\psi_2^0 - \psi_3^0) - 2\pi \\
 &= \psi_3^0 + P(\psi_2^0) + 2P(\psi_3^0) - P(\psi_2^0 - \psi_3^0) \\
 &= ((CA)_0) + P((BA)_0) + 2P((CA)_0) - P((BA)_0 - (CA)_0)
 \end{aligned}$$

Hence, if we set $x = BA$ and $y = CA$, we obtain the system

$$\begin{cases} x_1 = x_0 + 2P(x_0) + P(y_0) + P(x_0 - y_0) \\ y_1 = x_0 + P(x_0) + 2P(y_0) - P(x_0 - y_0). \end{cases}$$